

Polarization bremsstrahlung in a backward direction for medium structure diagnostics.

N. Nasonov[‡]¹, P. Zhukova¹, V. Sergienko²

¹ Laboratory of Radiation Physics, Belgorod State University, 14 Studencheskaya st., 308007 Belgorod, Russia

² Lebedev Physical Institute RAS, Moscow, Russia

Abstract. Possibilities to elaborate the new energy dispersive methods of the diagnostics of a medium atomic structure based on the polarization bremsstrahlung from relativistic electrons moving in a sample are analyzed in the paper. The method of radial density of atoms measuring in a weakly ordered medium is proposed in the paper as well as the method of cluster size determination in small grained medium.

Keywords: Polarization bremsstrahlung; Relativistic electrons; Radial density of atoms; Cluster size.

1. Introduction

When a fast charged particle moves through a dense medium it can emit electromagnetic waves due to the scattering of the particle Coulomb field by medium atoms. The distinctive property of the emission being discussed, known as the polarization bremsstrahlung (PB) [1, 2, 3], consists in the strong dependence of its characteristics on inter-atomic correlations in the target. This property opens the possibility to use PB for medium atomic structure diagnostics [4]. Since the spectrum of initial virtual photons associated with incident particle Coulomb field is wide enough, the spectral measurements of scattered photons are more convenient for the structure diagnostics on the base of PB. Such variant of X-ray diagnostics, known as EDXD (energy dispersive X-ray diffraction) [5, 6, 7], requires a well determined spectrum of primary photons. It should be noted in this connection that the use of PB for the diagnostics has an advantage consisting in the possibility to calculate exactly the spectrum of primary virtual photons. One further advantage of this approach connects with the possibility to elaborate the method of structure diagnostics with high space resolution. Indeed, the problem of a primary electron beam focusing on the sample by equipments of an ordinary magnetic optics is incomparably less than that for X-ray beam.

The suggestion to use PB for atomic structure diagnostics was verified by experiments, performed in the last few years. The measurements of the distances between atomic planes in polycrystalline targets have been realized experimentally on the base of PB from electrons with energies of about units MeV [8, 9, 10]. The possibility to determine texture in polycrystals by PB from 150 MeV electrons was demonstrated at the experiment [11]. The method of mosaic crystal diagnostics on the base of PB and the method of a nanocluster size measuring in small grained media have been recently proposed [12].

It should be noted that many crystallographic planes in a polycrystalline target make the contribution to PB yield simultaneously in the form of Bragg reflexes. The number and positions of such reflexes in total spectrum depend strongly on the observation angle between directions of an incident electron beam and diffracted photon fluxes. It is significant that reflexes can overlap and hence the accuracy of measurements is determined by the spectral width of these reflexes. Generally the value of PB peak width $\Delta\omega$ is inverse proportional to Lorentz factor of an emitting electron γ , so that the energy resolution of the method under consideration increases with increasing γ . Unique possibility to increase the energy resolution in the process of polycrystal diagnostics is connected with coherent PB peaks emitted in a backward direction relative to the electron velocity [13]. It has been shown in [13], that $\Delta\omega$ for such anomalous peaks is proportional to γ^{-2} and so these peaks are of interest for diagnostics tasks.

It is significant that the analogous peaks occur in the process of coherent PB from relativistic electrons moving in a single crystal [14, 15] (coherent part of PB in a single crystal is identical to well known parametric X-ray radiation [16, 17, 18]). Experimental studies of parametric X-ray radiation peaks emitted to backward direction relative to

an emitting electron velocity have demonstrated that the spectral width of these peaks ranges up to about tens MeV [15].

Our paper is devoted to the advancement of approach [13]. Possibilities to use backward PB peaks for the diagnostics of ordered in part media are the subject for our studies. New method of the diagnostics of short-range order in weakly ordered medium based on above PB peaks is elaborated in the next section of the paper. We discuss in section 3 the new method of cluster size measurement on the base of backward PB. Our conclusions are presented in section 4.

Relativistic system of units $\hbar = c = 1$ is used in the paper.

2. Relativistic electron PB to backward direction. Study of short-range order in weakly ordered medium

Let us consider the spectral-angular characteristics of PB photons emitted by relativistic electrons crossing a thin solid target starting from Maxwell equations for Fourier transform of excited electric field

$$(k^2 - \omega^2)\mathbf{E}_{\omega\mathbf{k}} - \mathbf{k}(\mathbf{k} \cdot \mathbf{E}_{\omega\mathbf{k}}) = 4\pi i\omega\mathbf{J}_{\omega\mathbf{k}} + \frac{i\omega e}{2\pi^2}\mathbf{V}\delta(\omega - \mathbf{k} \cdot \mathbf{V}), \quad (1)$$

Here the last item in the right side of (1) describes the current density of a fast electron, \mathbf{J} is the induced current density of medium electrons, determined within the frame of dipole approximation [3] by the equations

$$4\pi i\omega\mathbf{J}_{\omega\mathbf{k}} = \omega^2 \int d^3k' G(\mathbf{k}' - \mathbf{k})\mathbf{E}_{\omega\mathbf{k}'}, \quad (2)$$

$$G = \frac{1}{2\pi^2} \frac{\alpha_0(\omega)}{1 + (\mathbf{k}')^2 - \mathbf{k}^2 R^2} \sum_l e^{i(\mathbf{k}' - \mathbf{k})\mathbf{r}_l}, \quad \alpha_0(\omega) = \frac{e^2}{m} \sum_{n \geq 1} \frac{f_{n0}}{\omega_{n0}^2 - \omega^2},$$

where R is the screening radius in Fermi-Thomas atom model (the simplest model with exponential screening is used in our calculations), summation in (2) is performed over all atoms in the target, \mathbf{r}_l is the coordinate of l -th atom, $\alpha_0(\omega)$ is the ordinary dipole polarizability of an atom.

The function G describes both refraction and scattering of photons in the target. It is convenient for the further analysis to separate G into averaged over coordinates of all atoms and accidental components

$$G = \bar{G} + \tilde{G}, \quad \bar{G} = \langle G \rangle = 4\pi n_0 \alpha_0(\omega) \delta(\mathbf{k}' - \mathbf{k}), \quad 4\pi n_0 \alpha_0(\omega) = \chi(\omega), \quad 1 + \chi(\omega) = \varepsilon(\omega), \quad (3)$$

so that the scattering of a fast electron Coulomb field will be described by \tilde{G} only. Here n_0 is the average density of atoms, $\chi(\omega)$ and $\varepsilon(\omega)$ are the dielectric susceptibility and permeability of the target respectively.

The solution of (1) should be determined by perturbation theory. Substituting (3) into (1) and representing the total field $\mathbf{E}_{\omega\mathbf{k}}$ as a sum of the electron Coulomb field $\mathbf{E}_{\omega\mathbf{k}}^{eq}$

and the emission field $\mathbf{E}_{\omega\mathbf{k}}^{rad}$ one can obtain in the first-order of \tilde{G} the following expression for $\mathbf{E}_{\omega\mathbf{k}}^{rad}$

$$E_{\omega\mathbf{k}}^{rad} = \frac{i\omega^3 e}{2\pi^2} \frac{1}{k^2 - \omega^2 \varepsilon} \int \frac{d^3 k'}{k'^2 - \omega^2 \varepsilon} \tilde{G}(\mathbf{k}' - \mathbf{k}) \left(\mathbf{V} - \frac{\mathbf{k}'}{\omega \varepsilon} - \mathbf{k} \frac{\mathbf{k} \cdot \mathbf{V} - \frac{\mathbf{k} \cdot \mathbf{k}'}{\omega \varepsilon}}{\omega^2 \varepsilon} \right) \delta(\omega - \mathbf{k}' \cdot \mathbf{V}) \quad (4)$$

Formula for the spectral-angular distribution of the number of emitted photons follows from (4) in the form

$$\omega \frac{dN}{d\omega d\Omega} = e^2 \omega^6 \int \frac{d^3 k_1}{k_1^2 + 2\omega\sqrt{\varepsilon}\mathbf{n}\mathbf{k}_1} \frac{d^3 k_2}{k_2^2 + 2\omega\sqrt{\varepsilon}\mathbf{n}\mathbf{k}_2} \langle \tilde{G}(\mathbf{k}_1) \tilde{G}^*(\mathbf{k}_2) \rangle \left[\left(\mathbf{V} - \frac{\mathbf{k}_1}{\omega \varepsilon} \right) \left(\mathbf{V} - \frac{\mathbf{k}_2}{\omega \varepsilon} \right) - \left(\mathbf{n}\mathbf{V} - \frac{\mathbf{n}\mathbf{k}_1}{\omega \varepsilon} \right) \left(\mathbf{n}\mathbf{V} - \frac{\mathbf{n}\mathbf{k}_2}{\omega \varepsilon} \right) \right] \delta(\omega(1 - \sqrt{\varepsilon}\mathbf{n}\mathbf{V}) - \mathbf{k}_1\mathbf{V}) \delta(\omega(1 - \sqrt{\varepsilon}\mathbf{n}\mathbf{V}) - \mathbf{k}_2\mathbf{V}), \quad (5)$$

where all interatomic correlations of interest to us are contained in the correlator $\langle \tilde{G}(\mathbf{k}_1) \tilde{G}^*(\mathbf{k}_2) \rangle$.

To show the possibility to use PB for study of short-range order in solids one should calculate above correlator using two-particle density $f_2(\mathbf{r}_l, \mathbf{r}_m)$ which may be presented as a sum $f_2(\mathbf{r}_l, \mathbf{r}_m) = f_1(r_l)f_1(r_m) + g_2(|\mathbf{r}_l - \mathbf{r}_m|)$, where $f_1 = 1/V$ is one-particle distribution function for a homogeneous target, V is the volume of this target, g_2 is the two-particle correlation function. The desired radial density is expressed in term of the correlation function by the formula $n_0 V^2 n(r) = n(r) - n_0$ [19]. Based on above considerations one can represent (5) in the form

$$\omega \frac{dN}{d\omega d\Omega} = \omega \frac{dN_0}{d\omega d\Omega} + \omega \frac{d\Delta N}{d\omega d\Omega}. \quad (6)$$

Here the first item in the right side describes PB generated independently on each atom of the target

$$\omega \frac{dN_0}{d\omega d\Omega} \simeq \frac{2Z^2 e^6}{\pi m^2} L n_0 \left| \frac{\omega^2}{\omega_p^2} \chi(\omega) \right|^2 \frac{1}{(1 + 4\omega^2 R^2)^2} \left(\ln \sqrt{\frac{1 + 4\omega^2 R^2}{\omega^2 R \rho^2}} - 1 \right), \quad (7)$$

where Z is the number of electrons in a target atom, L is the thickness of the target, ω_p is the plasma frequency, $\rho^2 = \gamma^{-2} + \omega_p^2/\omega^2$, γ is Lorentz factor of an emitting fast electron.

The last item in (6) describes an addition to PB caused by interatomic correlations

$$\omega \frac{d\Delta N}{d\omega d\Omega} = \frac{2Z^2 e^6}{m^2 \omega} L n_0 \left| \frac{\omega^2}{\omega_p^2} \chi(\omega) \right|^2 \int_1^\infty \frac{dx}{(1 + 4\omega^2 R^2 x^2)^2} \frac{x^2 - 1}{(x^2 - 1 + \frac{1}{4}\rho^2)^2} \times \int_0^\infty dr r (n(r) - n_0) \sin(2\omega r x) \quad (8)$$

It is important to keep in mind that the results (7) and (8) have been obtained to fit PB photons emitted in a backward direction relative to an emitting electron velocity.

This is of no concern for PB on a separate atom (7), since the angular distribution of PB on an atom is close to isotropic one. On the other hand, it is of fundamental importance in the task of $\omega \frac{d\Delta N}{d\omega d\Omega}$ determination on the base of the result (8). Indeed, the connection between Fourier transform of radial density $n(r)$ and the quantity $\omega \frac{d\Delta N}{d\omega d\Omega}$ is integral, but in conditions of PB in a backward direction under consideration this connection can be approximated by local one due to extremely small value of the width of the range of momentum transfer, as it follows immediately from the coefficient $(x^2-1)/(x^2-1+\rho^2/4)^2$ consisting in a very sharp peak with the width of the order of $\rho^2/4 \approx 1/4\gamma^2 \ll 1$. Since the effective values of in the integral (8) is in the region of a distance between atoms l , the variable x in the function $\sin(2\omega r x)$ is approximately equal to unity with the proviso that

$$\frac{1}{4}\omega l \rho^2 \approx \frac{1}{4}\omega l \gamma^{-2} \ll 1 \quad (9)$$

As a result the formula (8) takes the form

$$\begin{aligned} \omega \frac{d\Delta N}{d\omega d\Omega} &\approx A(\omega) \int_0^\infty dr r (n(r) - n_0) \sin(2\omega r) \\ A(\omega) &= \frac{2Z^2 e^6}{m^2 \omega} L n_0 \left| \frac{\omega^2}{\omega_p^2} \chi(\omega) \right|^2 \frac{1}{(1 + 4\omega^2 R^2)^2} \ln \frac{16}{\rho^2} \end{aligned} \quad (10)$$

Formulae (6), (7) and (8) allow one to determine the function of radial density $n(r)$. Indeed, since PB spectral-angular distribution $\omega \frac{dN}{d\omega d\Omega}$ is defined experimentally and the coefficient $A(\omega)$ is calculated by the formula (10) as well as the distribution $\omega \frac{dN_0}{d\omega d\Omega}$ is calculated by (7) one can determine $n(r)$ by Fourier integral

$$n(r) - n_0 = \frac{1}{r} \frac{4}{\pi} \int_0^\infty d\omega \sin(2\omega r) \frac{\omega \frac{dN}{d\omega d\Omega} - \omega \frac{dN_0}{d\omega d\Omega}}{A(\omega)}, \quad (11)$$

analogous to that used in the classical Zernicke - Prins approach [20], based on angular measurements of scattered by a sample quasi-monochromatic X-ray beam.

It is of first importance that the approach being proposed does not constitute a conceptual disadvantage of Z-P method consisting in the availability of a finite top limit in the Fourier integral. The indicated limit causes substantial distortions in the function $n(r)$. The absence of above distortions within the frame of our approach is caused by EDXD technique and the possibility to determine the spectrum of initial virtual photons exactly.

3. Diagnostics of cluster size in small grained medium by anomalous PB peak

The general formula (5) is applicable for targets with arbitrary atomic structures. Let us use this formula for an analysis of the possibility to measure a cluster size in small

grained medium on the base of PB. In order to calculate the correlator $\langle \tilde{G}(\mathbf{k}_1) \tilde{G}^*(\mathbf{k}_2) \rangle$ one should set the coordinates of atoms in the target \mathbf{r}_n by the formula

$$\mathbf{r}_n = \mathbf{R}_n + \mathbf{r}_{nl} + \mathbf{u}_{nl}, \quad (12)$$

where \mathbf{R}_n is the coordinate of n-th cluster, \mathbf{r}_{nl} is the coordinate of l-th atom in n-th cluster, \mathbf{u}_{nl} is the thermal displacement of this atom. Averaging over thermal displacements \mathbf{u}_{nl} , cluster sizes, forms and orientations leads to the following expression for the correlator:

$$\langle \tilde{G}(\mathbf{k}_1) \tilde{G}^*(\mathbf{k}_2) \rangle = \frac{2}{\pi} \frac{|\alpha_0(\omega)|^2}{(1 + k_1^2 R^2)^2} \left[n_0 (1 - e^{-k_1^2 u^2}) + n_S \left(\langle |S(\mathbf{k}_1)|^2 \rangle + |\langle S(\mathbf{k}_1) \rangle|^2 \int d^3r (n_c(r) - n_S) e^{-\mathbf{k}_1 \mathbf{r}} \right) e^{-k_1^2 u^2} \right] \delta(\mathbf{k}_1 - \mathbf{k}_2), \quad (13)$$

where u is the mean square amplitude of thermal vibrations of atoms, n_S is the density of clusters, $n_c(r)$ is the radial density of clusters, analogous to that in an amorphous medium, $\langle S(\mathbf{k}) \rangle \equiv \langle S_l(\mathbf{k}) \rangle$, $S_l(\mathbf{k}) = \sum_{n=1}^{N_l} \exp(i\mathbf{k}\mathbf{r}_{ln})$ is the structure factor of l-th cluster, containing N_l atoms.

Since $u \ll R$, the contribution of incoherent part of PB is strongly suppressed in (13) and hence PB spectral-angular distribution follows from (5) and (13) in the form

$$\omega \frac{dN^{coh}}{d\omega d\Omega} = \frac{Z^2 e^6}{\pi^2 m^2} L n_S \frac{|\omega^2 \chi(\omega)|^2}{\omega_p^2} \int \frac{d^3k}{(1 + k^2 R^2)^2} \frac{(\omega \mathbf{V} - \frac{\mathbf{k}}{\varepsilon})^2 - (\omega \mathbf{nV} - \frac{\mathbf{nk}}{\varepsilon})^2}{(k^2 + 2\omega \sqrt{\varepsilon} \mathbf{nk})^2} \times \left[\langle |S(\mathbf{k})|^2 \rangle + \frac{4\pi}{k} |\langle S(\mathbf{k}) \rangle|^2 \int_0^\infty dr r (n_c(r) - n_S) \sin(kr) \right] e^{-k^2 u^2} \delta(\omega(1 - \sqrt{\varepsilon} \mathbf{nV}) - \mathbf{kV}) \quad (14)$$

different from (6) by the availability of cluster structure factor $S(\mathbf{k})$, describing the coherent contribution of cluster atoms to PB yield. It is clear, that the quantity $\langle |S(\mathbf{k})|^2 \rangle$ depends on the module of k only. In conditions of relatively small cluster sizes under consideration (measurement of cluster size of the order of 10 nm holds the greatest interest) the above function comprises a peak with a maximum at the point $k = 10$. Amplitude of this peak increases with increasing in cluster size, but its width decreases. Since the peak being discussed describes the cluster as an entire object, the microscopic arrangement of atoms in the cluster is of no importance to study of cluster size and hence we will use a very simple model of cubic lattice. Bearing the fundamental properties of the diagnostics method being studied in mind we neglect inter-cluster correlations in (14) and consider the cluster as a cube with N_S atoms arranged along its verge, so that the full number of atoms in the cluster is equal to N_S^3 . Assume that a is the distance between neighboring atoms. As this takes place, the quantity $\langle |S(\mathbf{k})|^2 \rangle$ is given by the formula

$$\begin{aligned}
T(ka, N_S) &= 1 + \frac{6}{N_S} \sum_{j=1}^N (N_S - j) \eta(j) + \frac{12}{N_S^2} \sum_{j=1}^N (N_S - j) \sum_{l=1}^N (N_S - l) \eta(\sqrt{j^2 + l^2}) + \\
&\frac{8}{N_S^3} \sum_{j=1}^N (N_S - j) \sum_{l=1}^N (N_S - l) \sum_{p=1}^N (N_S - p) \eta(\sqrt{j^2 + l^2 + p^2}) \\
\eta(\sqrt{j^2 + l^2 + p^2}) &= \frac{\sin(ka\sqrt{j^2 + l^2 + p^2})}{ka\sqrt{j^2 + l^2 + p^2}}, \quad \langle |S(\mathbf{k})|^2 \rangle = N_S^3 T(ka, N_S)
\end{aligned} \tag{15}$$

The dependence $T(ka, N_S)$ presented in Fig.1 confirms completely above reasoning on the properties of cluster structure factor.

Let us consider now the basic idea of cluster size measuring on the base of coherent PB from relativistic electrons. First of all, it should be noted that the spectrum of coherent PB described by (14),(15) has a maximum. Indeed, the factor $|\frac{\omega^2}{\omega_p^2} \chi(\omega)|^2$ in (14) tends to zero with decreasing in ω within the small frequency range where the susceptibility $\chi(\omega)$ is approximately constant and hence PB spectrum is suppressed in small frequency range. On the other hand, coherent PB is suppressed in high frequency range, where the cluster structure factor decreases with increase in because of decreasing of coherent contribution of cluster atoms to the formation of PB yield. It is clear that the position of above maximum depends on the cluster size, determining the form of structure factor (see Fig.1). The performed analysis of the results (14) and (15) has shown that the frequency range where the maximum in question is realized depends strongly on the observation angle between an emitting electron velocity and the unit vector to the direction of emitted photon propagation. The most clear-cut dependence of above maximum position on the cluster size manifests for backward PB owing to extremely small width of the range of momentum transfer (in a similar way to that in the case of amorphous target), but the maximum is realized in small frequency range. A simple result follows from (14) and (15) in conditions under consideration

$$\begin{aligned}
\omega \frac{dN^{coh}}{d\omega d\Omega} &= \frac{2Z^2 e^6}{\pi m^2} L n_0 \left| \frac{\omega^2}{\omega_p^2} \chi(\omega) \right|^2 \int_1^\infty dx \frac{\exp(-4\omega^2 u^2 x^2)}{(1 + 4\omega^2 R^2 x^2)^2} x T(2\omega a x, N_S) \frac{x^2 - 1}{(x^2 - 1 + \rho^2/4)^2} \approx \\
&\frac{2Z^2 e^6}{\pi m^2} L n_0 \ln\left(\frac{4}{\rho}\right) \left| \frac{\omega^2}{\omega_p^2} \chi(\omega) \right|^2 T(2\omega a, N_S)
\end{aligned} \tag{16}$$

where the last formula must be used with care because its accuracy is about of 15-20 per cent.

It is well to bear in mind that the calculated term in the right side of the equation (16) which is compared with measured left side of this equation is not convenient for cluster size determination because of strong distortions contributed by the dispersion of dielectric susceptibility $\chi(\omega)$. Considerably more convenient for comparison with data function is defined as $Q(\omega a, N_S) = \omega^2 a^2 T(2\omega a, N_S)$.

The function $Q(\omega a, N_S)$ should be compared with experimental results by the formula

$$Q(\omega a, N_S) = \frac{\pi m^2}{2Z^2 e^6} \frac{\omega_p^2 a^2}{Ln_0 \ln(4/\rho)} \frac{\omega_p^2}{\omega^2} \frac{1}{|\chi(\omega)|^2} \omega \frac{dN^{coh}}{d\omega d\Omega} \quad (17)$$

The task of cluster size determination is solved by the selection of the parameter N_S equivalent to cluster size for good agreement between calculated function $Q(\omega)$ and measured quantity, given by the right side of the equation (17). It is clear, that more realistic results may be obtained within the frame of more general model of the target as an ensemble of clusters with different forms and sizes, but such analysis is beyond the scope of this paper.

High sensitivity of the function $Q(\omega)$ to cluster size is demonstrated by curves presented in Fig.2. An important point is that the desired cluster size is determined by the position of maximum in PB spectrum, which can be measured with accuracy substantially better than that for traditional measuring of the width of PB coherent peak.

Conclusions

The performed analysis shows the possibility to use collective effects in PB from relativistic electrons moving in a dense media for the target atomic structure diagnostics. PB in a backward direction is particularly appealing for the diagnostics because of unique small width of the range of momentum transfer in the emission process.

A new EDXD method of the diagnostics of radial density function for atoms in a weakly ordered medium on the base of relativistic electron PB in a backward direction is proposed. The desired function is reconstructed by the equation (11). The field of integration in this equation is not bounded from overhead and the spectrum of initial virtual photons associated with incident electron Coulomb field is well defined, which is why the desired function $n(r)$ is not distorted in distinction to Zernicke-Prins approach.

PB may be used for the measurement of cluster sizes in a small grained medium. The proposed method is based on one-to-one correspondence between the cluster size and the position of coherent maximum in PB spectrum caused by the scattering of incident electron Coulomb field by the cluster as an entire object. An important point is that PB in a backward direction is found to be proportional to average square of module of cluster structure factor. This circumstance allows one to determine the cluster size on the base of simple equation (18).

A conceptual sketch of the method being proposed is considered in this paper. The inclusion of a spread of cluster sizes and forms as well as inter-cluster correlations will allow one to realize substantially more realistic model for interpretations of observational data.

Acknowledgments

This work was accomplished in the context of both FCP of Russian Ministry of Education and Science and RFBR (grant:09-02-97528).

References

- [1] Amusia M et al. 1992 *Polarization Bremsstrahlung from Particles and Atoms* (New York: Plenum Press)
- [2] Korol A et al. 1997 *J.Phys.B:At.Mol.Opt.Phys.* **30** 1105-1150.
- [3] Korol A and Lyalin A and Solov'ev A 2004 *Polarization Bremsstrahlung* (St. Petersburg: St.PSPU publ) (In Russian).
- [4] Nasonov N 1998 *Nucl.Instr.Meth. B* **145** 19-24.
- [5] Coppens P., Cox D., Vieg E. and Robinson I.K. 1992 *Synchrotron Radiation Crystallography*. (Academic Press. London, San Diego, New York, Boston, Sydney, Tokio, Toronto). 316p.
- [6] Buras B. and Gerward L. 1995 *Techniques for X-rays In: International Tables for Crystallography* (Ed.by A.J.C. Wilson. IUCr: Dordrecht, Boston, London: Kluwer Academic Publishers) 84-87.
- [7] Clarck S.M. 2002 *Thirty years of energy dispersive powder diffraction* Crystallography Reviews. **8** 57-92.
- [8] Blazhevich S et al. 1999 *Phys.Lett. A* **254** 230.
- [9] Astapenko V., Kubankin A., Nasonov N. et al. 2006 *JETP Lett.* **84** 281-284.
- [10] Gostishchev N., Kubankin A., Nasonov N. et. al 2008 *Technical Physics Lett.* **34** 78-82.
- [11] Takabayashi Y et al. 2006 *Nucl.Instr.Meth. B* **243** 453.
- [12] Astapenko V and Gostishchev N and Zhukova P et al 2008 *Bulletin of the Russian Academy of Science:Physics* **6** 926-929.
- [13] Astapenko V and Nasonov N and Zhukova P 2007 *ZJ. Phys. B: At. Mol. Opt. Phys.* **40** 1-10.
- [14] Brenzinger K-H and Limburg B and Backe H et al. 1997 *Phys. Rev. Lett.* **79** 2462-2465.
- [15] Backe H and Ay C and Clawiter N et al. 2003 *Proc. Symp. Channeling-Bent Crystals-Radiation Processes* 41-58.
- [16] Baryshevsky V and Feranchuk I 1971 *Sov.Phys.JETP* **61** 944-948.
- [17] Garibian G and Yang S 1971 *Sov. Phys. JEPT* **61** 930-943.
- [18] Baryshevsky V and Feranchuk I and Ulyanenkov A 2005 *Parametric X-ray Radiation in Crystals. Theory, Experiment and Applications* (Springer. Berlin) 176 p.
- [19] James R. 1950 *Optical principles of the diffraction of X-rays* (Ed. L. Bragg. London:The crystalline state) **2**.
- [20] Zernicke F and Prins A 1927 *Zs. f. Phys.* **41** 184.

Figure captions

Figure 1.

Square of the module of cluster structure factor versus the momentum transfer, calculated for different cluster size.

Figure 2.

The position of the maximum of PB spectral peak versus the cluster size.

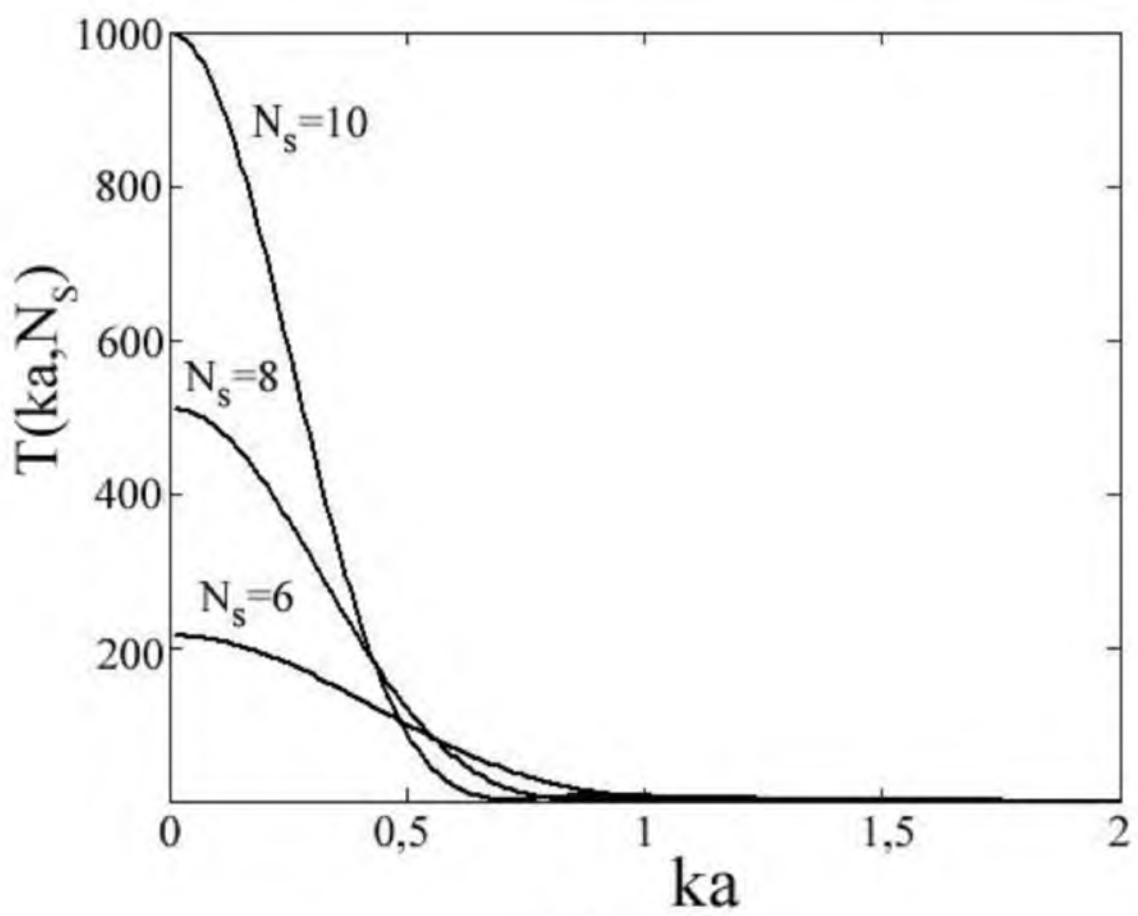


Fig.1

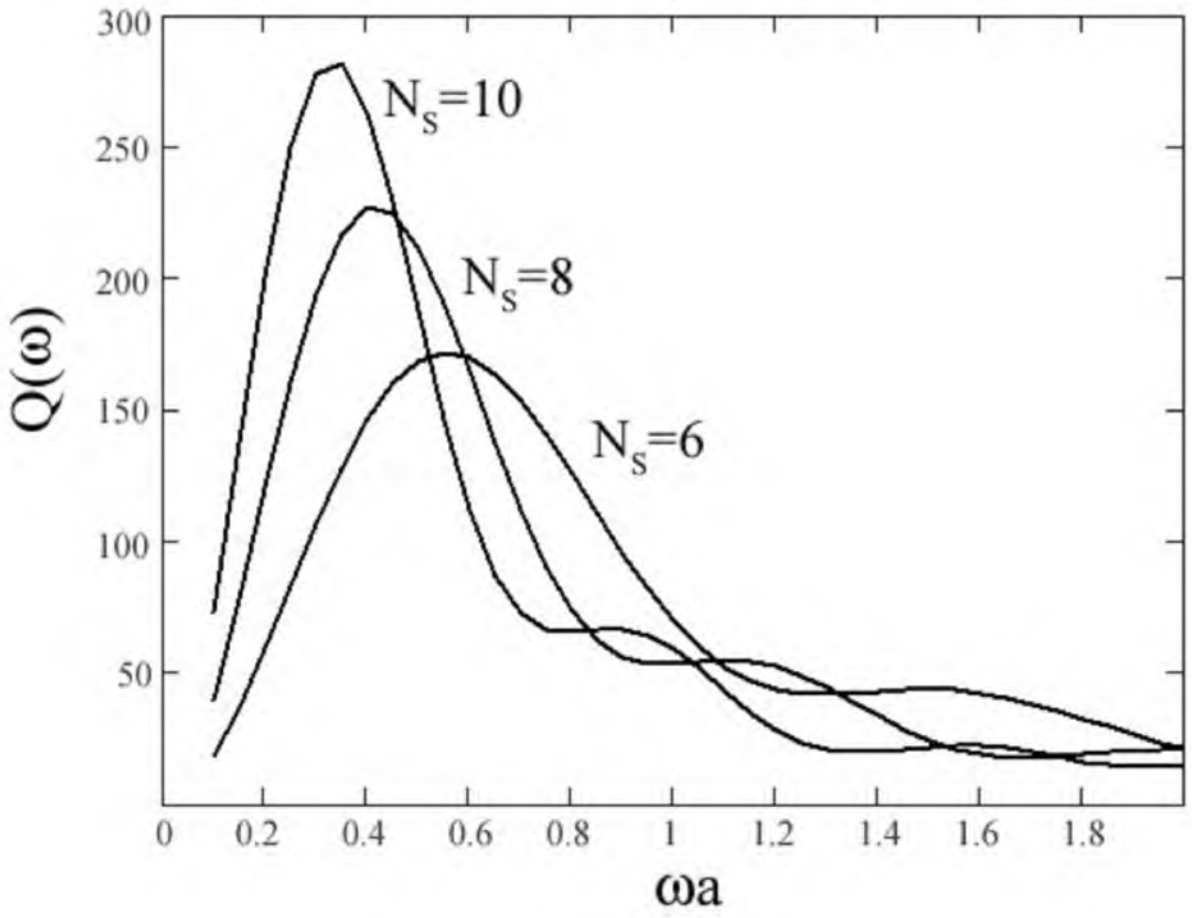


Fig.2